Design and Deployment of an Autonomous IoT-Based Medical Monitoring System for Military Operations in Infrastructure-Limited Environments

DAN TSHITAMBA MUTAMBAYI[1], MOANDA NDEKO MOSENGO[1], WITESYAVWIRWA VIANNEY KAMBALE[3], KYANDOGHERE KYAMAKYA[1,2]
[1]Faculté Polytechnique, Université de Kinshasa (UNIKIN),
Kinshasa, Democratic
REPUBLIC OF THE CONGO

[2]Institute for Smart Systems Technologies,
Universität Klagenfurt,
AUSTRIA

[3]Faculty of Information and Communication Technology,
Tshwane University of Technology,
Pretoria,
SOUTH AFRICA

Abstract: In conflict-affected and infrastructure-deficient areas, such as the eastern Democratic Republic of Congo (DRC), military troops face significant health hazards without reliable access to medical services or communication systems. This paper outlines the design and implementation of an autonomous Internet of Things (IoT)-based medical monitoring system that operates independently of internet access. The system incorporates low-power embedded technologies, such as the ESP32 WROOM-32UE microcontroller, DS18B20 temperature sensor, Polar H9 heart rate monitor, Neo-6M GPS, and SIM800L GSM module, to provide real-time monitoring of vital signs and geolocation of soldiers in the field. Data transmission occurs over SMS, guaranteeing uninterrupted functionality in faraway areas. The suggested system prioritizes energy efficiency, immediate reactivity, localized alarm production, and modular scalability. Thorough system testing and deployment simulations demonstrate its ability to enhance wartime situational awareness and facilitate prompt medical interventions for frontline personnel.

Key-Words: - Wearable Device, monitoring, medical, military, GSM, Embedded System, SMS.

Received: April 19, 2025. Revised: July 26, 2025. Accepted: September 7, 2025. Published: December 31, 2025.

1 Introduction

1.1 Background and Motivation

In the Democratic Republic of Congo (DRC), particularly in the eastern region, military troops have significant problems. These regions, characterized by persistent security instability, impose exceedingly severe living circumstances. Soldiers stationed on the front lines face considerable health hazards, including fatigue, infectious diseases, cardiovascular conditions, and grave injuries. Geographic inaccessibility places a soldier in a medical emergency at significant danger. In this context, marked by the precarious healthcare situation in the Democratic Republic of Congo (DRC), especially for military personnel in conflict zones, it is imperative to investigate the various challenges concerning healthcare accessibility and quality for the Congolese armed forces. The inadequate medical infrastructure requires a scientific and technological strategy for developing a remote, real-time health monitoring system for each soldier deployed in these conditions. In the absence of such a system, how can the efficacy of frontline operations be guaranteed if the military command center is unable to consistently acquire physiological data for each soldier, thus failing to identify in real-time which personnel necessitate immediate replacement or evacuation based on their precise location and physical condition? Furthermore, how can medical aid be efficiently prioritized and allocated to meet the persistent health requirements of each soldier? Consequently, particular emphasis should be placed on ongoing health surveillance methodologies. A monitoring system must be established to provide precise, real-time data on each soldier within their unit, facilitating the early identification of emergencies and a swift response to critical incidents.

1.2 Problem statement and Research Questions

Military operations in isolated and conflict-ridden areas often lack the necessary infrastructure for

prompt medical assistance and situational awareness regarding the health status of deployed personnel. In the eastern DRC, inadequate healthcare facilities, deficient network infrastructure, and extensive operational terrain intensify this problem, resulting in avoidable health-related deaths and operational inefficiencies. Conventional health surveillance systems depend significantly on internet access and centralized cloud servers, which are impractical in such settings. An autonomous, lightweight, and field-ready IoT solution is needed for real-time monitoring and decision-making that is independent of internet-based platforms. Consequently, this study delineates the subsequent research questions (RQs):

- RQ-1: How can an autonomous IoT-based system effectively monitor and communicate critical health and geolocation data of military personnel without internet connectivity?
- RQ-2: What are the ideal sensor configurations and system designs to guarantee minimal power consumption, resilience, and real-time performance in remote operational environments?
- RQ-3: How does the proposed system compare with current telemedicine or wearable monitoring systems in terms of scalability, latency, and efficacy in infrastructure-limited settings?

The subsequent sections of this work are structured as follows. Section II provides a concise overview of cutting-edge IoT-based health monitoring systems and telemedicine in conflict areas. Section III delineates the system architecture. Section IV delineates the specifics of implementation. Section V delineates the experimental configuration and assessment. Section VI presents an analysis of the findings. Ultimately, Section VII summarizes the report and delineates avenues for future research.

2 Brief Review of State-of-the-Art of IoT-based Health Monitoring Systems and Telemedicine in Conflict Zones

Multiple studies on wearable systems highlight their rapid developmental potential across various domains, particularly within the realm of Internet of Things (IoT) technologies. These technologies are particularly relevant for patient monitoring, enabling the remote acquisition and analysis of vital parameters using sensor-based systems. Advancements in this field are propelled by the downsizing of sensors and the integration of autonomous, connected embedded systems. These systems rely on integrated microsystems that comprise sensors linked to microcontrollers. They are engineered to gather, process, and transmit data utilizing wireless communication protocols. The gathered data can be relayed to a remote server or dispatched via SMS, accessible through various user interfaces, including smartphones, tablets, or laptops, thus serving as conduits to a centralized analysis and processing system.

3 System Design of the Remote Medical Monitoring System

The architecture of the proposed remote medical monitoring system is influenced by the following constraints: lack of internet connectivity in conflict zones, restricted access to power sources, and the necessity for real-time health tracking and geolocation. An energy-efficient modular architecture was implemented to tackle these difficulties.

3.1 Assessment of specific requirements for monitoring vital signs

Vital signs are crucial markers for evaluating an individual's overall health status. They assist in identifying possible physiological dysfunctions and directing clinical investigations to achieve an appropriate diagnosis, [1]. These factors can be examined, quantified, and monitored to assess the body's correct functioning. Any substantial deviation from regular readings should be regarded as a warning signal necessitating urgent attention, [2]. Among these essential indicators, we have the following:

- Heart Rate,
- The respiratory frequency,
- The body temperature,
- Blood pressure,
- Oxygen saturation.

The standard ranges of these indicators may fluctuate based on age, gender, weight, physical activity, and overall health, [2]. In light of the subject's intricacy, we shall concentrate on two critical vital signs pertinent to our study: body temperature and heart rate. The decision to focus our study exclusively on body temperature and heart rate is based on the fact that these two measurements are direct indicators of an individual's metabolic, cardiovascular, and immunological state.

3.1.1 The body temperature

Body temperature is a crucial metric for evaluating the body's thermal balance and overall health condition. Any substantial variation from normal values may signify an underlying issue, rendering it one of the most straightforward methods to assess a patient's condition, [2]. Despite natural diurnal temperature variations, the human body possesses intrinsic regulation mechanisms, a process known as homeostasis, which is indicative of its homeothermic characteristics. Body temperature is a fluctuating characteristic that varies from individual to individual. The temperature ranges from 36°C to 37.5°C and is considered normal (apyrexia, or the absence of fever). Any deviation from this range is termed as

- Hypothermia: $< 35.5\,^{\circ}\mathrm{C}$. Mild hypothermia manifests within the temperature range of 34 °C to 35 °C. The condition is marked by a conscious patient exhibiting shivering, pallor, coldness, and piloerection, accompanied by increased blood pressure. Moderate hypothermia occurs when body temperature falls between 34°C and 32°C. Chilly and dry skin, continuous shivering, speech impairments, reduced voluntary movements, and disorientation mark this phase. Severe hypothermia occurs below 32°C, indicating the threshold for critical hypothermia. This temperature decline may result in cardiac arrest or a significant decrease in heart rate, diminishing to 1 to 2 beats per minute, rendering it practically undetectable. The pulse becomes imperceptible, accompanied by bilateral pupil dilation (mydriasis) and generalized muscular rigidity.
- Subfebrile or febrile condition: 37.5°C to 38°C This temperature range is mildly elevated, although it remains beneath the threshold classified as a fever. Side effects of medication, stress, exhaustion, or hormonal imbalances, including hyperthyroidism or other endocrine diseases, might induce it.
- Hyperthermia: Exceeding 38°C This phenomenon is termed fever, characterized by an increase in body temperature typically resulting from an infection. This phenomenon arises from the secretion of pyrogenic chemicals by immune cells and injured tissues, which influence the hypothalamus to elevate body temperature. It is crucial to recognize that such an elevation may also result from heatstroke, frequently induced by extended exposure to elevated ambient temperatures, particularly in susceptible or dehydrated individuals, such as those exposed to sunlight, [1]. Numerous factors can influence body temperature, including physical activity, stress, gender, digestion, and circadian rhythms. The latter denotes a biological cycle of approximately 24 hours that governs the body's physiological functions in response to external stimuli, such as light, and internal elements, including hormones.

3.1.2 The heart rate

Heart rate denotes the frequency of heartbeats per minute (beats per minute, bpm). It is a crucial indicator of cardiovascular health and overall well-being. This measurement assesses the heart's ability to circulate blood and respond to the body's physiological needs. Heart rate is often confused with pulse or rhythm due to widespread misapplication of these terms. Heart rhythm denotes the consistency of heartbeats, which may be classified as regular, exhibiting a uniform pattern with consistent intervals, or irregular, marked by erratic beats with varied intervals. The pulse denotes the frequency of pulsations detected per minute in an artery, reflecting the blood flow propelled by the heart. Every heartbeat produces a pressure wave in the arteries, recognized as a pulse. The pulse rate typically corresponds with the heart rate, except in some pathological conditions, such as pulse deficiency, where some heartbeats fail to generate a detectable pulse. Normal heart rate readings are contingent upon age, physical activity level, and general health status. At repose, these values often reside within a well-established reference range:

- Adult or adolescent (over 14 years old): 60 to 100 BPM;
- Child (under 14 years old): 70 to 140 BPM;
- Infant (under 2 years): 100 to 160 BPM;
- Newborn (less than 1 month): 120 to 160 BPM, [1].

All requirements must be evaluated in conjunction with specific indications, including the typical pulse rate. It is crucial to recognize that highly trained endurance athletes often exhibit a resting heart rate below 60 bpm, a phenomenon known as physiological bradycardia, which is indicative of their cardiovascular system's superior efficiency. The theoretical maximal heart rate (MHR) during physical exercise is determined by subtracting age from 220 (e.g., 220 – 28 years = 192). This, however, does not consider individual variances associated with fitness level, gender, or other characteristics. The estimation by Tanaka, Monahan, and Seals offers enhanced precision. Maximum Heart Rate (MHR) = 208 -

(0.7 × age). Numerous more factors affect heart rate, including:

- Heart rate fluctuates throughout 24 hours, governed by circadian rhythms. It often diminishes during sleep, owing to the predominance of the parasympathetic nervous system, and then rises upon awakening, reaching its zenith around noon or early afternoon.
- The heart rate may see a modest elevation postprandially, when the heart circulates additional blood to the digestive system for nutritional absorption.
- Elevated ambient temperatures can result in an increased heart rate, promoting heat dissipation through improved blood circulation.
- Stress stimulates the sympathetic nervous system, resulting in an elevation of heart rate through three primary mechanisms: Neurological (stimulation of the brain through the hypothalamus), chemical (release of catecholamines, including adrenaline and noradrenaline), and physical (direct physiological alterations, such as increased blood flow).

3.2 Functional description of the electronic components of the system

3.2.1 Microcontroller ESP32 WROOM-32UE

Figure 1 illustrates the ESP32 WROOM-32UE microcontroller from the ESP32 family designed by Espressif Systems, developed by Espressif Systems, that incorporates integrated Wi-Fi and Bluetooth connectivity, making it an ideal choice for Internet of Things (IoT) applications. This variant features a USB-C port and an IPEX connector for an external antenna, facilitating straightforward operation, enhanced RF connectivity, and effortless integration into diverse prototypes or projects, [3].

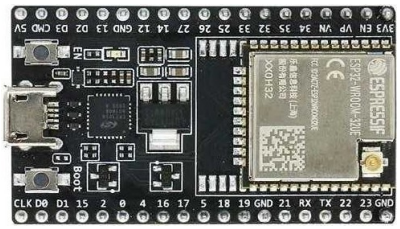

Fig. 1: ESP32 WROOM-32UE

3.2.2 SIM800L GSM Module

The SIM800L, as illustrated in the Figure 2, is a compact and multifunctional GSM/GPRS module designed to enable communication for embedded systems via cellular networks. It can transmit SMS, initiate phone calls, connect to the internet via GPRS, and facilitate Bluetooth communication, [4]. This module is frequently utilized in IoT projects, remote monitoring systems, and mobile communication applications, [4].

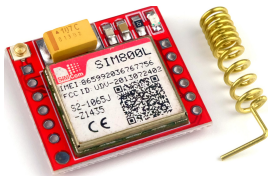

Fig. 2: SIM800L GSM module

3.2.3 The DS18B20 temperature sensor

The DS18B20 is a prevalent digital temperature sensor recognized for its accuracy, durability, and capability to communicate using a single wire (One-Wire protocol). Figure 3 illustrates the DS18B20 used in this project, an ideal component for measuring temperatures in electronics and IoT projects, [5].

Fig. 3: DS18B20 temperature sensor

3.2.4 Polar H9 Heart Rate Sensor

The Polar H9 is a precise and dependable heart rate monitor intended for athletic and medical use. This sensor as shown in Figure 4, utilizing ECG (electrocardiogram) technology, has a precision of ±1 bpm under dynamic situations. It functions through a chest strap fitted with electrodes that directly measure the heart's electrical activity, ensuring superior accuracy compared to optical sensors, [6].

Fig. 4: Polar H9

3.2.5 GPS neo-6M module

The GPS neo-6M module shown in Figure 5 is a compact and high-performance GPS receiver, equipped with an integrated neo-6M chip that provides accurate positioning and navigation data. This module is frequently utilized in various applications, including drones, vehicular geolocation systems, and personal navigation devices, [7].

Fig. 5: GPS neo-6M

3.2.6 Passive buzzer

Figure 6 illustrates a passive buzzer, an electronic component capable of generating sounds when periodic electrical signals are applied to it. In contrast to an active buzzer, a passive buzzer requires an external input frequency to generate sound, thereby allowing complete control over the tone and duration of the audio output, [8].

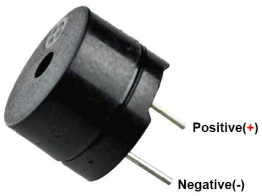

Fig. 6: passive buzzer

3.2.7 LED

An LED (Light Emitting Diode) as shown in Figure 7 is an electronic component that emits light when a current passes through it, [9].

Fig. 7: Red LED

3.2.8 Lithium-Ion (Li-Ion) Battery 3.7V 2000mAh

A 3.7V 2000mAh Lithium-Ion (Li-Ion) battery, as shown in Figure 8, is a commonly used component in embedded electronic systems due to its high energy density and rechargeable capability.

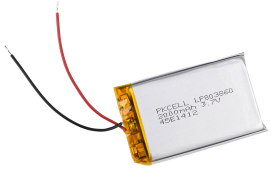

Fig. 8: 3.7V 2000mAh battery

3.3 Design and Mathematical modeling of the system's operating parameters and their interactions with the microcontroller

The hardware design of the system, aligned with the project's aims, is founded on the ESP32 WROOM-32UE, which manages and processes data from the sensors. For continuous monitoring of physiological parameters, the Polar H9 heart rate sensor and DS18B20 temperature probe have been selected. In the event of critical threshold breaches, the passive buzzer and LED are activated to signal a local alert. Additionally, the Neo-6M GPS module is integrated to include the patient's geographical location in case of an emergency.

3.3.1 Mathematical modeling of the DS18B20 sensor

The DS18B20 uses a temperature sensor based on a thermally sensitive diode, [5]. It leverages the relationship between the voltage across the PN junction and the temperature. It is known that the diode equation is given by:

$$I = I_s \left(e^{\frac{qV_d}{kT}} - 1 \right) \tag{1}$$

- I is the current flowing through the diode,
- I_s is the reverse saturation current,
- V_d is the voltage across the diode,
- q is the charge of the electron ($1.6 \times 10^{-19} C$),
- k is the Boltzmann constant ($1.38 \times 10^{-23} J/K$),
- T is the absolute temperature in Kelvin, [10].

For moderate voltages ($V_d \approx 0.6V$ for a silicon diode), we can approximate:

$$I \approx I_s e^{\frac{qV_d}{kT}} \tag{2}$$

To find the expression for V_d as a function of T, take the logarithm of both sides:

$$\ln I = \ln I_s + \frac{qV_d}{kT} \tag{3}$$

Isolating V_d:

$$V_d = \frac{kT}{q} \ln\left(\frac{I}{I_s}\right) \tag{4}$$

This equation shows that the diode voltage decreases as the temperature increases. Consider a reference temperature T_0 and a voltage V_0:

$$V_0 = \frac{kT_0}{q} \ln\left(\frac{I}{I_s}\right) \tag{5}$$

If the temperature varies slightly around T_0, then $T = T_0 + \Delta T$. A first-order approximation gives:

$$V_d(T) \approx V_d(T_0) + \left(\frac{dV_d}{dT}\right)_{T_0} (T - T_0) \tag{6}$$

We differentiate V_d with respect to T:

$$\frac{dV_d}{dT} = \frac{k}{q} \ln\left(\frac{I}{I_s}\right) + \frac{kT}{q} \cdot \frac{1}{I} \cdot \frac{dI}{dT} \tag{7}$$

If the current I is constant:

$$\frac{dI}{dT} \approx 0 \tag{8}$$

Thus:

$$\frac{dV_d}{dT} \approx \frac{k}{q} \ln\left(\frac{I}{I_s}\right) \tag{9}$$

For a silicon diode:

$$\frac{dV_d}{dT} \approx -2 \text{ mV/°C} \tag{10}$$

This coefficient is denoted α, which gives:

$$V(T) = V_0 + \alpha \cdot (T - T_0) \tag{11}$$

where:

- V_0 is the voltage measured at a reference temperature T_0,
- α is the thermal coefficient (≈2mV/°C for a silicon diode),
- $T - T_0$ is the temperature variation.

This equation explains why a PN junction can be used as a temperature sensor: the voltage decreases linearly with increasing temperature. The DS18B20 converts the measured voltage into a 16-bit binary value through an Analog-to-Digital Converter (ADC), and the resolution is programmable between 9 and 12 bits, [5]. It is essential to note that the higher the resolution, the more precise the conversion; however, it also requires more time. Each bit represents:

- 9 bits → 0.5°C per unit;
- 10 bits → 0.25°C per unit;
- 11 bits → 0.125°C per unit;
- 12 bits → 0.0625°C per unit (default value).

In this context, the formula for converting raw data is given by:

$$T = \frac{D}{16} \tag{12}$$

where:

- D is the 16-bit raw value received,
- T is the temperature in °C.

Once the temperature is converted, the DS18B20 sends it to the ESP32 via the 1-Wire protocol, which operates as follows:

1. The ESP32 sends a conversion request to the sensor via a command (`0x44`);
2. The DS18B20 measures the temperature, performs the ADC conversion, and stores the value in its internal RAM;
3. The ESP32 sends a read request (`0xBE`);
4. The DS18B20 transmits the temperature in the form of 16 bits (two bytes), [3], [5].
   - Byte 1 = Least significant bits,
   - Byte 2 = Most significant bits,
5. The ESP32 reconstructs the 16-bit data and applies the temperature conversion.

3.3.2 Mathematical modeling of the Polar H9 sensor

The heart is an electrophysiological organ that generates electrical signals that trigger muscle contraction. An electrical signal generated by the heart follows a well-defined cycle known as the PQRST wave, observable on an electrocardiogram (ECG). The QRS wave represents ventricular depolarization, i.e., the electrical impulse that commands the contraction of the heart. The Polar H9 detects these impulses by capturing the R peaks of the QRS signal, which are the most pronounced in the QRS complex. Each heartbeat generates an R peak,

and the duration between two successive R peaks is called the RR interval, given by the equation:

$$RR = t_{R2} - t_{R1} \tag{13}$$

where:

- RR is the interval between two beats in seconds (s),
- t_{R2} and t_{R1} are the times at which the successive R peaks appear, [11].

The RR interval represents the period of the heart signal. Since heart rate is defined as the inverse of the RR period, its equation is obtained by:

$$FC = \frac{1}{RR} \tag{14}$$

To express heart rate in beats per minute (BPM), we must convert seconds to minutes:

$$FC = \frac{60}{RR} \tag{15}$$

where:

- FC is the heart rate in BPM,
- RR is the interval in seconds, [11].

To improve the stability of the measurement, several RR intervals are averaged. The heart rate is then defined as:

$$FC = \frac{60}{\frac{1}{N}\sum_{i=1}^{N} RR_i} \tag{16}$$

where:

- N is the number of cycles considered,
- RR_i is the RR interval of the i the beat, [11].

The Polar H9 transmits the RR values via Bluetooth Low Energy (BLE) to the ESP32, and the latter stores the RR values as an unsigned 16-bit integer (uint16):

$$RR\_BLE = \lfloor RR \times 1024 \rfloor \tag{17}$$

where:

- RR is expressed in seconds,
- RR_{BLE} is the value transmitted via BLE in units of 1/1024 seconds.

Once the RR_{BLE} data is received and stored, the ESP32 performs the inverse conversions:

$$RR = \frac{RR_{BLE}}{1024} \tag{18}$$

where:

- RR is the RR interval in seconds.

Since the formula obtains the heart rate:

$$FC = \frac{60}{RR} \tag{19}$$

3.3.3 Mathematical modeling of the GPS neo-6M module

The Neo-6M GPS module allows the determination of geographical position (latitude and longitude), as well as speed and time. It relies on signals transmitted by at least four satellites of the GPS (Global Positioning System) network and applies precise mathematical calculations to estimate the position of a receiver, [7]. The GPS used in this project is based on a method called trilateration. The principle of trilateration relies on the fact that the GPS receiver (Neo-6M module) receives signals from multiple satellites, and each satellite i transmits:

1. Its transmission timestamp t_{e_i},
2. Its known coordinates (x_i, y_i, z_i),
3. The GPS signal traveling at the speed of light c, [12].

The GPS receiver measures the arrival time t_r and calculates the distance d_i to each satellite:

$$d_i = c \cdot (t_r - t_{e_i}) \tag{20}$$

where:

- d_i is the distance between satellite i and the receiver (in meters),
- $c = 3.0 \times 10^8$ m/s is the speed of light,
- t_r is the reception time,
- t_{e_i} is the signal transmission time.

It should be noted that the GPS module's clock is not perfectly synchronized with the satellites' clocks, so a timing error b must be considered. The objective is to determine the position (x, y, z) of the GPS module in a 3D Cartesian coordinate system by solving a system of nonlinear equations based on the distance to each satellite.

Each satellite i has a known position (x_i, y_i, z_i), and we know that:

$$\sqrt{(x - x_i)^2 + (y - y_i)^2 + (z - z_i)^2} = d_i + b \tag{21}$$

Squaring both sides gives:

$$(x - x_i)^2 + (y - y_i)^2 + (z - z_i)^2 = (d_i + b)^2 \tag{22}$$

Using four satellites, we obtain four equations for four unknowns (x, y, z, b):

$$(x - x_1)^2 + (y - y_1)^2 + (z - z_1)^2 = (d_1 + b)^2 \tag{23}$$

$$(x - x_2)^2 + (y - y_2)^2 + (z - z_2)^2 = (d_2 + b)^2 \tag{24}$$

$$(x-x_3)^2+(y-y_3)^2+(z-z_3)^2=(d_3+b)^2 \quad (25)$$

$$(x-x_4)^2+(y-y_4)^2+(z-z_4)^2=(d_4+b)^2 \quad (26)$$

To solve the problem algebraically, we expand each equation:

$$x^2-2xx_i+x_i^2+y^2-2yy_i+y_i^2+z^2-2zz_i+z_i^2=d_i^2+2d_ib+b^2 \quad (27)$$

To simplify, we subtract the first equation from the three others:

$$-2x(x_i-x_1)-2y(y_i-y_1)-2z(z_i-z_1)=(d_1^2-d_i^2) -(x_1^2-x_i^2)-(y_1^2-y_i^2)-(z_1^2-z_i^2)+2b(d_1-d_i) \quad (28)$$

We then obtain a linear system in the form:

$$A\cdot X=B \quad (29)$$

where:

- A is a 3×3 matrix containing the coefficients of the linearized equations,
- X is the vector of unknowns (x,y,z,b),
- B is the vector of constants.

This system can be solved using Cramer's matrix method:

$$X=A^{-1}B \quad (30)$$

Thus, the GPS coordinates are obtained as follows:

$$\lambda=\tan^{-1}\left(\frac{y}{x}\right) \quad (31)$$

$$\phi=\tan^{-1}\left(\frac{z+e^2R_E\sin(\phi_0)}{\sqrt{x^2+y^2}}\right) \quad (32)$$

$$h=\frac{\sqrt{x^2+y^2}}{\cos(\phi)}-R_E \quad (33)$$

where:

- $R_E=6378137$ m is the mean radius of the Earth,
- e is the eccentricity of the Earth,
- ϕ_0 is an initial estimate of the latitude.

The NEO-6M GPS module sends the coordinates to the ESP32 via a UART (Universal Asynchronous Receiver Transmitter) serial communication in the NMEA 0183 (National Marine Electronics Association) GPS data format, [7]. Each message begins with an identifier followed by values separated by commas. The ESP32 receives the NMEA sentences and must extract and convert the data into usable values. Therefore, the ESP32 must extract the values and convert the data into decimal degrees. The GPS coordinates are provided in degrees and minutes ($ddmm.mmmm$), [7].

3.3.4 Mathematical modeling of the LED as an alarm actuator

We will mathematically explain the operation of the red LED used in the system. It is important to recall that the red LED cannot operate directly at 3.3 V (the ESP32 supply voltage). It requires a series resistor to limit the current. We will calculate:

- The current flowing through the LED;
- The power consumption;
- The impact of the current on the LED's lifespan;
- The effect of PWM control on brightness.

Using Ohm's Law, we can determine the current I_{LED} flowing through the LED:

$$I_{LED}=\frac{V_{source}-V_{LED}}{R} \quad (34)$$

where:

- $V_{source}=3.3V$ is the ESP32 supply voltage;
- $V_{LED}=2V$ is the forward voltage of the red LED;
- $R=220\Omega$ is the current-limiting resistor (we selected ($R=220\Omega$) because our system is intended to consume less energy and ensure a longer lifespan).

Substituting the values:

$$I_{LED}=\frac{3.3V-2V}{220\Omega}=\frac{1.3V}{220\Omega} \quad (35)$$

$$I_{LED}=5.91mA \quad (36)$$

Therefore, the current flowing through the LED is approximately 5.91 mA, which is well below the typical 20 mA rating, ensuring optimized brightness.

The power consumed by the LED is:

$$P=V_{LED}\times I_{LED} \quad (37)$$

$$P=2V\times 5.91mA=11.82mW \quad (38)$$

The power dissipated by the resistor is given by:

$$P_R=R\times I_{LED}^2 \quad (39)$$

$$P_R=220\Omega\times(5.91mA)^2 \quad (40)$$

$$P_R=220\times(0.00591)^2=7.68mW \quad (41)$$

We conclude that the LED consumes (11.82mW), which is very low. The resistor dissipates (7.68mW), so it does not heat up significantly.

LEDs are typically designed to operate with currents ranging from 10 mA to 20 mA. With (5.91mA), we are well below the 20 mA limit, which implies:

- A significantly increased LED lifespan;
- Optimized LED brightness.

The ESP32 can adjust the LED brightness using PWM (Pulse Width Modulation). The average current I_{avg} is given by:

$$I_{\text{avg}} = I_{LED} \times D \tag{42}$$

where:

- D is the duty cycle ($0 \leq D \leq 1$);
- $I_{LED} = 5.91mA$ is the maximum current.

PWM examples:

- (D = 100%) $\rightarrow I_{\text{avg}} = 5.91mA$ (LED at full brightness);
- (D = 50%) $\rightarrow I_{\text{avg}} = 2.95mA$ (LED half brightness);
- (D = 10%) $\rightarrow I_{\text{avg}} = 0.59mA$ (LED dimly lit).

We choose full brightness since it is already optimized in our configuration.

3.3.5 Mathematical modeling of passive Buzzer as an alarm actuator

A passive buzzer operates like a piezoelectric speaker, producing sound in response to an alternating electrical signal (PWM), [8]. The ESP32 sends a square wave signal at a defined frequency to generate a sound at the corresponding frequency.

The buzzer is driven by a square wave signal of frequency f_{PWM}, which is also the frequency of the emitted sound:

$$f_{\text{sound}} = f_{\text{PWM}} \tag{43}$$

where:

- f_{sound} is the frequency of the produced sound in Hertz (Hz),
- f_{PWM} is the frequency of the PWM signal applied to the buzzer.

3.3.6 Mathematical modeling of the GSM SIM800L module

The SIM800L module is a GSM device utilized for transmitting and receiving SMS messages. The ESP32 manages it through the UART interface, utilizing AT instructions. This module employs the RSSI (Received Signal Strength Indicator), which denotes the strength of the signal received by a GSM module, [4]. The SIM800L quantifies the RSSI as a raw integer value between 0 and 31. The strength of a radio transmission is often quantified in dBm, a logarithmic measure defined by:

$$P_{\text{dBm}} = 10 \log_{10} \left(\frac{P}{1 \text{ mW}} \right) \tag{44}$$

- P_{dBm} is the signal power in dBm,
- P is the absolute power in milliwatts (mW).

Thus, the ESP32 sends AT commands to the SIM800L via the UART interface. The transmission rate is defined by:

$$B = \frac{1}{T_{\text{bit}}} \tag{45}$$

where:

- B is the baud rate in bits per second (bps),
- T_{bit} is the duration of a single bit.

The SIM800L typically operates at 9600 bps, and each SMS character is encoded using 7 bits. Therefore, for an SMS of $C = 160$ characters, we have:

$$N = 160 \times 7 = 1120 \text{ bits} \tag{46}$$

The transmission time of the SMS between the ESP32 and the SIM800L is:

$$T_{\text{ESP32}} = \frac{N}{B} = \frac{1120}{9600} = 0.1167 \text{ s} \tag{47}$$

An SMS of 160 characters is transmitted to the SIM800L via UART in approximately 0.12 seconds. Upon receiving the signal, the module must communicate it to the network. Prior to transmission, an SMS is encoded in Protocol Data Unit (PDU) format, which increases the message size.

3.3.7 System power supply

Ensuring a sustainable power supply for an onboard medical monitoring device represents a significant challenge. Designed to be autonomous and compact, it is essential to adopt an optimized solution that effectively balances performance, energy consumption, and cost. As a result, we chose a power architecture based on 3.7 V, 2000 mAh

Li-Ion batteries, combined with dynamic energy management strategies, such as deep sleep, which we implemented on the ESP32 WROOM-32UE microcontroller. We will connect our two batteries in parallel to maintain the same voltage while increasing the total capacity. We remind you that our batteries have the same nominal voltage, capacity, and technology, which justifies our decision to connect them in parallel. When two identical batteries are connected in parallel:

- The total voltage remains $V = 3.7V$
- The total capacity is the sum of the individual capacities:

$$Q_{\text{total}} = Q_1 + Q_2 \tag{48}$$

$$Q_{\text{total}} = 2000mAh + 2000mAh = 4000mAh \tag{49}$$

The representative current draw and corresponding power consumption of each module (for the operating modes used in the autonomy estimate) are summarized in Table 1 (Appendix).

1. Stored Energy Calculation

$$E_{\text{total}} = V \times Q_{\text{total}} \tag{50}$$

Convert Q_{total} into Ampere-hours:

$$Q_{\text{total}} = 4000mAh = 4Ah \tag{51}$$

$$E_{\text{total}} = 3.7V \times 4Ah = 14.8Wh \tag{52}$$

Therefore, the total available energy is 14.8 Wh (53.28 kJ).

2. T
3. The module power values used in the autonomy estimation are taken from Table 1 (Appendix).
4. Total Power Calculation

$$P_{\text{total}} = P_{\text{ESP32}} + P_{\text{Polar H9}} + P_{\text{DS18B20}} + P_{\text{LED}} + P_{\text{Buzzer}} + P_{\text{SIM800L}} + P_{\text{GPS}} \tag{53}$$

$$P_{\text{total}} = 0.888 + 0.0495 + 0.00495 + 0.0195 + 0.099 + 0.555 + 0.1485 \tag{54}$$

$$P_{\text{total}} = 1.76445W \tag{55}$$

So the total power consumption is approximately 1.76 W when all modules are active.

5. Battery Runtime

$$t_{\text{autonomie}} = \frac{E_{\text{total}}}{P_{\text{total}}} \tag{56}$$

$$t_{\text{autonomie}} = \frac{14.8Wh}{1.76W} \tag{57}$$

$$t_{\text{autonomie}} \approx 8.41h \tag{58}$$

4 Implementation of the Remote Medical Monitoring System

Following the mathematical modeling of the system, we proceed to its hardware and software implementation by combining the various components and ensuring their effective communication with the ESP32 WROOM-32UE microcontroller. The modules' interconnection depends on clearly defined communication interfaces:

1. Transmission of location and alert data
   - The NEO-6M GPS module communicates with the ESP32 via the UART interface on GPIO pins 26 and 27,
   - The SIM800L GSM module transmits alert SMS messages via UART communication on GPIO pins 16 and 17.
2. Acquisition of physiological parameters
   - The DS18B20 temperature sensor, based on the One-Wire protocol, is connected to GPIO 4 of the ESP32 to acquire the soldier's body temperature,
   - The Polar H9 heart rate sensor uses Bluetooth Low Energy (BLE) to exchange its data with the ESP32.
3. Visual and auditory alert system
   - The passive buzzer, used to emit sound alarms in case of abnormalities, is connected to GPIO 15,
   - The alert LED, serving as a visual indicator, is controlled by GPIO 22.
4. System power supply
   - Two 3.7V 2000 mAh Li-Ion batteries are connected in parallel, maintaining the same voltage while increasing the total capacity, thereby extending the device autonomy,

- The ESP32 and SIM800L are powered directly by the batteries, while the other components (GPS, DS18B20, Polar H9, LED, and buzzer) draw power from the ESP32 3.3V pin,
- All circuit grounds are common to ensure a proper electrical reference and avoid potential differences.

Figure 9 shows the wiring diagram of our project, illustrating the internal functionality of the electronic device as explained above.

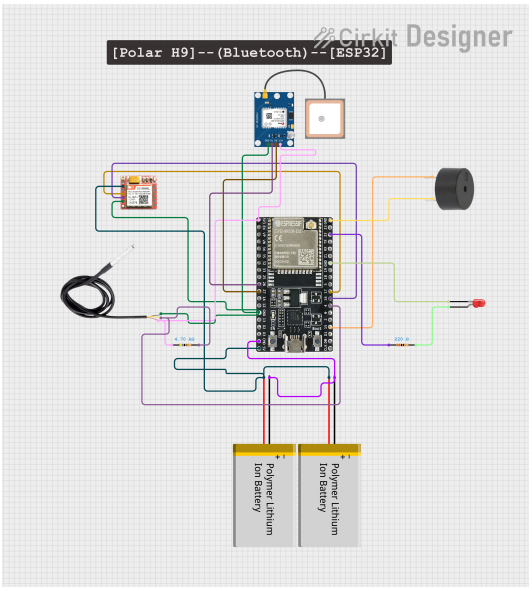

Fig. 9: Wiring diagram of the project using Circuit Designer software

4.1 Acquisition of results

1. Figure 10 gives us the precise heart rate values in BPM from the Polar H9 sensor

2. The body temperature values in °C measured with the DS18B20 sensor are shown in Figure 11

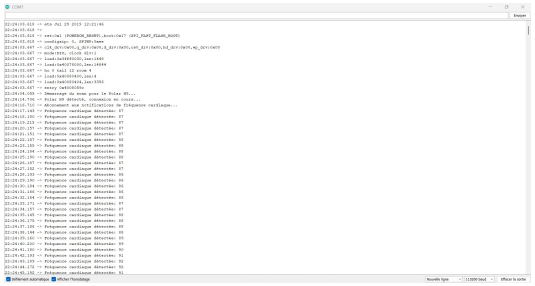

Fig. 10: Heart rate of a male volunteer measured in BPM

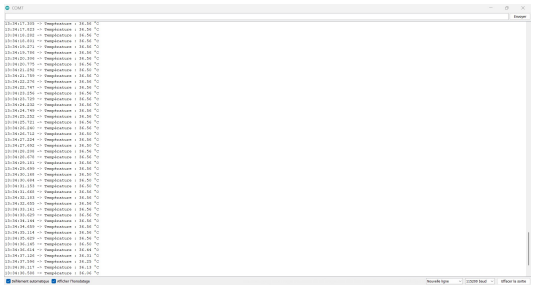

Fig. 11: Body temperature of a male volunteer measured in °C

3. The neo-6M GPS module, as shown in Figure 12, provided us with location coordinates with considerable accuracy.

Fig. 12: GPS coordinates obtained using the trilateration method

4.2 Remote data transmission via the GSM SIM800L module

We executed the complete hardware and software design process, guaranteeing the dependability and precision of the data transmitted by the project's critical components. Within this architecture, the temperature and heart rate sensors interface with the ESP32 microprocessor, which is tasked with obtaining real-time data. The ESP32 not only processes and analyzes sensor data but also facilitates remote data transmission with the SIM800L communication module. This transmission is crucial to the health monitoring system, enabling operators and medical personnel to obtain data immediately and thereby facilitating the swift identification of physiological irregularities. Figure 13 shows the ESP32 serial monitor output (Arduino IDE), validating the real-time acquisition and formatting of sensor and GPS data prior to transmission. Figure 14 shows a representative SMS received on a mobile phone via the SIM800L, confirming end-to-end GSM delivery of the monitoring data.

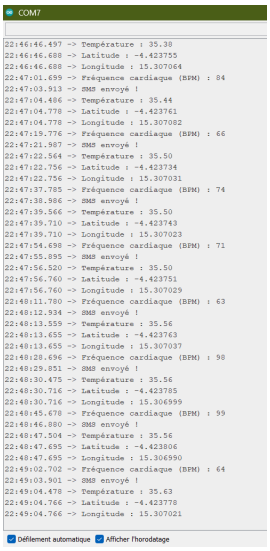

Fig. 13: Data collection and transmission by the ESP32, visualized through the Arduino IDE serial monitor

5 Experimental Setup and Evaluation

5.1 Analysis of data from the DS18B20 sensor

The DS18B20 sensor provides temperature measurements at regular intervals. Here, we analyze its accuracy by determining several key statistical parameters.

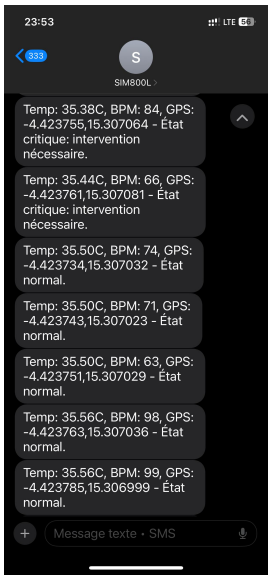

Fig. 14: Reception of data via GSM on a mobile phone

Number of Measurements The total number of measurements is:

$$N = 46 \tag{59}$$

Average Temperature The average of the recorded temperatures is given by:

$$\bar{T} = \frac{\sum_{i=1}^{N} T_i}{N} \tag{60}$$

where T_i represents each recorded temperature value. Substituting the values:

$$\bar{T} \approx 36.01^{\circ}\text{C} \tag{61}$$

Temperature Standard Deviation The standard deviation is calculated as:

$$\sigma_T = \sqrt{\frac{\sum_{i=1}^{N} (T_i - \bar{T})^2}{N}} \tag{62}$$

Which gives:

$$\sigma_T \approx 0.18^{\circ}\text{C} \tag{63}$$

Mean Absolute Error The mean absolute error is calculated as:

$$\mu_T = \frac{\sum_{i=1}^{N} |T_i - \bar{T}|}{N} \tag{64}$$

Applying the values:

$$\mu_T \approx 0.13^{\circ}\text{C} \tag{65}$$

Sensor Accuracy The sensor accuracy is defined as:

$$\text{Accuracy} = \left(1 - \frac{\mu_T}{\bar{T}}\right) \times 100 \tag{66}$$

Which gives:

$$\text{Accuracy} \approx 99.63\% \tag{67}$$

The results show that the DS18B20 sensor offers an accuracy of 99.63%, with low standard deviation and mean absolute error. This indicates that the measurements are consistent and reliable for monitoring the body temperature of a soldier deployed on the front line.

5.2 Analysis of data from the Polar H9 sensor

We analyze the heart rate (BPM) data collected to determine the accuracy of the sensor used. The calculated metrics include standard deviation, mean error, and overall accuracy.

Number of Measurements The total number of measurements collected is:

$$N = \text{Total number of data points} = 200 \tag{68}$$

Average Heart Rate The average BPM value is given by:

$$\bar{X} = \frac{1}{N}\sum_{i=1}^{N} X_i \tag{69}$$

where X_i represents each recorded BPM value.

$$\bar{X} = 89.5BPM \tag{70}$$

BPM Standard Deviation The standard deviation is calculated as:

$$\sigma_{BPM} = \sqrt{\frac{1}{N}\sum_{i=1}^{N}(X_i - \bar{X})^2} \tag{71}$$

$$\sigma_{BPM} = 2.3BPM \tag{72}$$

It represents the dispersion of the measured values around the mean.

Mean Error The mean absolute error is defined as:

$$\mu_{BPM} = \frac{1}{N}\sum_{i=1}^{N} |X_i - \bar{X}| \tag{73}$$

$$\mu_{BPM} = 1.8BPM \tag{74}$$

This measures the average deviation of each measurement from the overall mean.

Sensor Accuracy in Our System The accuracy is defined as:

$$P_{HR} = 100 \times \left(1 - \frac{\sigma}{\bar{X}}\right)\% \tag{75}$$

$$P_{HR} = 97.43\% \tag{76}$$

The results show that the sensor used has good accuracy (97.43%), a value that adequately meets the project's requirements.

5.3 Analysis of data from the GPS neo-6M module

In this analysis, we evaluate the accuracy of GPS measurements using a dataset consisting of multiple latitude and longitude points. We apply the Haversine formula to calculate the distances between successive points and derive the system's accuracy.

Definition of Terms

- $N = 42$: Number of measures,
- ϕ : Latitude in radians,
- λ : Longitude in radians,
- R: Mean radius of the Earth (6371 km),
- d: Distance between two GPS points,
- σ_d: Standard deviation of GPS distances,
- μ_d: Mean GPS positional error,
- P: GPS accuracy,
- N: Total number of measurements.

Calculation of Distance Between Two GPS Points The distance between two consecutive GPS points is calculated using the Haversine formula:

$$d = 2R \cdot \arcsin\left(\sqrt{\begin{array}{l}\sin^2\left(\frac{\Delta\phi}{2}\right) \\ + \cos(\phi_1)\cdot\cos(\phi_2)\cdot\sin^2\left(\frac{\Delta\lambda}{2}\right)\end{array}}\right) \tag{77}$$

where:

- $\Delta\phi = \phi_2 - \phi_1$,
- $\Delta\lambda = \lambda_2 - \lambda_1$.

Calculation of the Standard Deviation of GPS Distances The standard deviation of the distances is given by:

$$\sigma_d = \sqrt{\frac{1}{N}\sum_{i=1}^{N}(d_i - \bar{d})^2} \tag{78}$$

where:

- d_i : Distance between point i and point $i+1$,
- $\bar{d}$: Mean of the calculated distances.

Calculation of the Mean GPS Positional Error The mean positional error is calculated as:

$$\mu_d = \frac{1}{N}\sum_{i=1}^{N} d_i \tag{79}$$

Calculation of GPS Accuracy The GPS accuracy is defined as:

$$P_{GPS} = 2 \cdot \sigma_d \tag{80}$$

$$\bar{d} = 0.97m \tag{81}$$

$$\sigma_d = 0.54m \tag{82}$$

$$\mu_d = 0.97m \tag{83}$$

$$P_{GPS} = 1.08m \tag{84}$$

6 Discussion of Results and Future Work

Assessing a medical monitoring and localization system requires a comprehensive analysis of the collected data to confirm its reliability and effectiveness. This chapter analyzes the outcomes derived from the medical monitoring and GPS geolocation system implemented for soldiers stationed in the conflict areas of the eastern Democratic Republic of the Congo (DRC). The analysis seeks to evaluate the precision and efficacy of the employed sensors, identify any constraints, and provide enhancements to optimize the system.

In a context characterized by violent conflicts, real-time monitoring of soldiers' vital signs and geolocation presents a considerable challenge to secure their safety and enhance operational efficiency. The dependability of the data supplied by this system might be critical, directly affecting survival probabilities during confrontations, reconnaissance missions, or rescue operations. This chapter will discuss:

1. Detailed analysis of the sensors' performance, emphasizing accuracy, reliability, and behavior in a combat environment;
2. Identified limitations during testing and their impact on military operations;
3. Potential improvements and advanced technologies that could be integrated to enhance the system's field viability.

6.1 Accuracy and Effectiveness of the DS18B20 Temperature Sensor

The DS18B20 sensor was incorporated into the system to monitor soldiers' body temperature in real-time. Accurate temperature monitoring is essential, since it facilitates the identification of dehydration, hypothermia, or infections, especially in the harsh environments of battle zones.

6.1.1 Results and Data Analysis

A series of 46 measurements was conducted on a volunteer, and Table 2 summarizes the key statistics.

Table 2. Analysis of body temperature measurements

Parameter	Calculated Value
Number of measurements (N)	46
Average Temperature (T)	36.01°C
Standard Deviation (σ_T)	0.18°C
Mean Absolute Error (μ_T)	0.13°C
Calculated Accuracy	99.63%

The DS18B20 sensor demonstrates very high accuracy (99.63%), which is acceptable for field medical monitoring of soldiers.

6.1.2 Challenges and Limitations

- **Limited Responsiveness**: The sensor shows a slight delay ($\tilde{0}.75$ s) in updating values, which may be negligible given the 25-second transmission interval. However, rapid health deterioration in severely injured soldiers might require faster updates for optimal diagnostics.
- **Environmental Influence**: Exposure to high ambient temperatures (above 40°C) can slightly skew measurements due to thermal transfer.

6.1.3 Potential Improvements and Technological Alternatives

- Integration of a machine learning-based correction algorithm: A model trained on

real-world conditions could reduce the mean error from 0.13°C to an even more precise value.

- Kalman filtering: This would smooth the data and eliminate outliers, providing maximum accuracy in body temperature measurements.

6.2 Analysis of Polar H9 Heart Rate Sensor Accuracy

The Polar H9 sensor was integrated into the project due to its reputation for precision and reliability in both sports and military environments.

6.2.1 Results and Accuracy Calculations

The accuracy study involved comparing several subsequent measurements using statistical approaches, including standard deviation, mean error, and overall accuracy. Table 3 encapsulates the findings.

Table 3. Heart rate measurement analysis results

Parameter	Calculated Value
Number of measurements (N)	200
Average BPM ($\bar{X}$)	89.5 BPM
Standard Deviation (σ)	2.3 BPM
Mean Error (μ_{BPM})	1.8 BPM
Accuracy (P_{HR})	97.43%

The tests indicate that the Polar H9 achieves an accuracy of approximately 97.43%, making it highly suitable for military applications. Although this sensor operates effectively in practical situations, additional enhancements could improve the analysis and optimize the utility of the gathered data.

6.2.2 Possible Improvements

1. Integration of a cardiac trend analysis algorithm
   - A machine learning-based approach could detect cardiac anomalies (tachycardia, bradycardia, atrial fibrillation) in real-time;
   - The algorithm could assign fatigue and stress scores to each soldier based on their physiological history.
2. Advanced notification system
   - Currently, alerts are triggered based on fixed thresholds. An improvement would be an adaptive system based on context and individual physiological variations.
   - For example, a soldier on a nocturnal reconnaissance mission will naturally have a lower heart rate than during active engagement. Dynamic analysis would differentiate normal fatigue from critical situations.

6.3 Analysis of Neo-6M GPS Module Accuracy

Locating soldiers on the field is critical, particularly during ambushes, night operations, or rescue missions. The Neo-6M GPS module was tested to evaluate its reliability.

6.3.1 Results and Accuracy Calculations

The evaluation was performed by comparing multiple successive points and calculating the distance between them using the **Haversine formula. Table 4 summarizes the results.

Table 4. Neo-6M GPS module accuracy

Parameter	Calculated Value
Average distance between GPS points (d)	0.97 m
Standard deviation of distances (σ_d)	0.54 m
Mean positional error (μ_d)	0.97 m
Calculated GPS accuracy (P_{GPS})	1.08 m

The Neo-6M GPS module attained an average accuracy of 1.08 meters, which is highly satisfactory in open terrain. Nonetheless, precision may diminish in metropolitan environments due to obstructions and interferences, such as these structures. Our project primarily focuses on open terrains; nonetheless, enhancements are necessary to attain more precision.

6.3.2 Possible Improvements

- Advanced Kalman filtering to correct GPS positions
  - Uses previous measurements to predict position,
  - Can significantly improve precision to a few centimeters.
- Median filtering
  - Smooths fluctuations caused by interference or measurement errors by taking the median of a set of successive values, eliminating outliers,
  - Improves GPS trajectory by correcting erratic jumps in GPS paths due to measurement errors.

The analysis of the results shows that the developed system is reliable and accurate, providing satisfactory performance for operational use in military environments. Nevertheless, some limitations need to be addressed to improve robustness and ensure long-term durability. By integrating the advanced technologies and methods proposed above, the system could reach higher levels of precision and performance, ensuring even more effective and secure monitoring for soldiers in the field.

7 Conclusion

This study focused on the design, implementation, and evaluation of a medical monitoring and military localization system in war zones. This research occurs in a situation where armed troops, especially those stationed in the eastern Democratic Republic of Congo, encounter considerable difficulties regarding health monitoring and on-ground cooperation. This project utilizes technologies that integrate biometric sensors, GPS localization, and real-time data transfer to significantly enhance operational management and military safety.

The technological approach adopted relies on the integration of several modules:

- Biometric sensors (temperature and heart rate) to monitor vital signs,
- A GPS module for precise soldier localization on the field,
- A microcontroller ensuring data centralization and processing,
- A GSM module guaranteeing the transmission of information to a command center.

The experimental findings indicated that the devised system achieves an average GPS accuracy of 1.08 meters, which is generally adequate for tracking in open environments. The DS18B20 temperature sensor and Polar H9 heart rate sensor exhibited accuracies of 99.63% and 97.43%, respectively, thereby ensuring dependable monitoring of the soldiers' physiological data.

However, some limitations were identified, including:

- The GPS module's susceptibility to environmental interference, particularly in urban settings or beneath forest canopies,
- The device's power consumption necessitates improved methods to prolong autonomy during missions,
- The absence of a sophisticated correction technique to enhance GPS and physiological measurements.

To improve system performance, several perspectives can be considered:

- Employing sophisticated Kalman filtering to enhance the precision of GPS coordinates and reduce location inaccuracies,
- Energy optimization through the integration of intelligent power management and the utilization of high-capacity batteries,
- Creating an innovative analytical interface that enables military command to visualize real-time data and predict key scenarios,
- Incorporating sophisticated technologies, including artificial intelligence, to evaluate physiological data and predict potential health hazards for soldiers.

This study has conclusively demonstrated the feasibility of integrating embedded technologies with communication systems to enhance health monitoring and soldier location in combat zones. The real-time utilization of this data enhances soldiers' protection and facilitates tactical decision-making in hazardous settings. This project establishes a foundation for novel research avenues, namely in enhancing portable devices intended for military applications and tailoring them to asymmetric warfare scenarios, where information responsiveness and precision are paramount. Recognizing that all human efforts may contain flaws, we are receptive to scientific collaboration aimed at enhancing our work and ensuring it aligns with the established initial objectives.

References

[1] *Health assessment module 3: Vital signs & assessment techniques notes*, Studocu lecture notes for Exp: Pharmacology (Rpl) (NUR 3992), University of North Florida, Accessed: January 12, 2025. [Online]. Available: https://www.studocu.com/en-us/document/university-of-north-florida/exp-pharmacology-rpl/health-assessment-module-3-notes/39905702.

[2] M. Khan, *Nursing skills (vital signs)*, Scribd document (PDF), Accessed: January 2, 2025. [Online]. Available: https://www.scribd.com/document/642716864/Nursing-Skills-Vital-Signs-1-pdf.

[3] E. Systems, *Esp32-wroom-32e and esp32-wroom-32ue datasheet*, Accessed: October 1, 2024, Espressif Systems, 2023. [Online]. Available: https://www.espressif.com/sites/default/files/documentation/esp32-wroom-32e_esp32-wroom-32ue_datasheet_en.pdf.

[4] Shanghai SIMCom Wireless Solutions Ltd., *SIM800L Hardware Design*, Version 1.00, Document Control ID: SIM800L_Hardware_Design_V1.00, Release date: 2013-08-20. Accessed: February 1, 2025., Shanghai SIMCom Wireless Solutions Ltd., Aug. 2013. [Online]. Available: https://www.makerhero.com/img/files/download/Datasheet_SIM800L.pdf.

[5] Maxim Integrated Products, Inc., *DS18B20: Programmable resolution 1-Wire digital thermometer*, Rev. 6, 19-7487, Rev. 6; 7/19. Accessed: January 22, 2025., Maxim Integrated Products, Inc., Jul. 2019. [Online]. Available: https://www.analog.com/media/en/technical-documentation/data-sheets/ds18b20.pdf.

[6] Polar Electro Oy, *Polar H9 Heart Rate Sensor: User Manual*, 2.0 (EN), Document marked "2.0 EN 12/2025". Accessed: January 22, 2025., Polar Electro Oy, Dec. 2025. [Online]. Available: https://support.polar.com/e_manuals/h9-heart-rate-sensor/polar-h9-user-manual-english/manual.pdf.

[7] u-blox AG, *NEO-6: u-blox 6 GPS Modules Data Sheet*, Revision E, GPS.G6-HW-09005-E, Revision E dated 05/12/2011. Accessed: December 2, 2024., u-blox AG, Dec. 2011. [Online]. Available: https://content.u-blox.com/sites/default/files/products/documents/NEO-6_DataSheet_%28GPS.G6-HW-09005%29.pdf.

[8] TDK Corporation, *Ps series piezoelectric buzzers datasheet*, 007-01, Issue date: May 2011. Accessed: December 23, 2024, TDK Corporation, 2011. [Online]. Available: https://www.mouser.com/datasheet/2/400/ef532_ps-13444.pdf.

[9] WAH WANG HOLDINGS (HONG KONG) CO., LTD., *Ww05a3srp4-n: 5mm super bright red led (5a3 series) datasheet*, Version 2.1. Accessed: December 27, 2024, Wah Wang Holdings (Hong Kong) Co., Ltd., 2012. [Online]. Available: https://supply24.online/doc/datasheet/Optoelektronika/Svetodiodi/THT-svetodiodi/THT-svetodiodi-5mm/WW05A3SRP4-N/WW05A3SRP4-N28ver229.pdf.

[10] R. L. Boylestad and L. Nashelsky, *Electronic Devices and Circuit Theory*, 11th ed. Upper Saddle River, NJ: Pearson Prentice Hall, 2013, ISBN: 978-0-13-262226-4. [Online]. Available: https://repositori.mypolycc.edu.my/jspui/handle/123456789/4961.

[11] P. Maccallini, *Introduction to the analysis of heart rate variability from 5-minute recordings*, Online manuscript (PDF, 41 pages), Dated February 2024 on the manuscript page. Accessed: January 23, 2025, Feb. 2024. [Online]. Available: https://www.academia.edu/114904479/Introduction_to_the_analysis_of_heart_rate_variability_from_5_minute_recordings.

[12] E. Chaniotakis, *Trilateration and the gps*, Educational resource hosted by School of the Future; page submitted on December 17, 2015. Accessed: January 23, 2025, Ellinogermaniki Agogi, Research and Development Department, Dec. 2015. [Online]. Available: https://www.schoolofthefuture.eu/sites/default/files/gps_0.pdf.

Contribution of Individual Authors to the Creation of a Scientific Article (Ghostwriting Policy) The authors equally contributed in the present research, at all stages from the formulation of the problem to the final findings and solution.

Sources of Funding for Research Presented in a Scientific Article or Scientific Article Itself No funding was received for conducting this study.

Conflicts of Interest The authors have no conflicts of interest to declare.

APPENDIX

Table 1. Electrical consumption of the modules

Module	Current Consumption (mA)	Voltage (V)	Power (W)
ESP32 (WiFi active)	240mA	3.7V	$0.888W$
Polar H9 (BLE)	15mA	3.3V	$0.0495W$
DS18B20 (Active measurement)	1.5mA	3.3V	$0.00495W$
Red LED (100%)	5.91mA	3.3V	$0.0195W$
Passive Buzzer (50%)	30mA	3.3V	$0.099W$
SIM800L (SMS)	150mA	3.7V	$0.555W$
GPS NEO-6M (Tracking)	45mA	3.3V	$0.1485W$